

Faster Model Predictive Control via Self-Supervised Initialization Learning

Zhaoxin Li¹, Letian Chen¹, Rohan Paleja², Subramanya Nagesh Rao³, Matthew Gombolay¹

Abstract—Optimization for robot control tasks, spanning various methodologies, includes Model Predictive Control (MPC). However, the complexity of the system, such as non-convex and non-differentiable cost functions and prolonged planning horizons often drastically increases the computation time, limiting MPC’s real-world applicability. Prior works in speeding up the optimization have limitations on solving convex problem and generalizing to hold out domains. To overcome this challenge, we develop a novel framework aiming at expediting optimization processes. In our framework, we combine offline self-supervised learning and online fine-tuning through reinforcement learning to improve the control performance and reduce optimization time. We demonstrate the effectiveness of our method on a novel, challenging Formula-1-track driving task, achieving 3.9% higher performance in optimization time and 3.6% higher performance in tracking accuracy on challenging holdout tracks.

I. INTRODUCTION

Iterative control optimization algorithms have been widely adopted to control the dynamic systems such as autonomous vehicles [1, 2, 3, 4], aircraft [5, 6], humanoid robots [7], etc. These optimization paradigms often entail dealing with complex systems featuring constraints, high dimensional solution space, and sudden state changes. Due to the inherent complexity of such systems, finding a good-enough solution (within some tolerance) in a single attempt can be exceedingly challenging for the optimizer. Consequently, solvers adopt an iterative approach to gradually converge towards a satisfactory solution. Typically, these algorithms start with an initial guess of the control inputs (e.g., joint accelerations) and employs solvers to iteratively minimize the cost function [8]. However, the optimization process can be significantly complicated by factors, such as the non-convex and non-differentiable cost function [9, 10]. Consequently, the optimization time of MPC is typically a bottleneck in its real-world applications [11, 12, 13, 14]. Addressing this challenge is paramount for enhancing the practical utility of MPC in various domains.

Given the iterative nature of the solvers used in optimization for robot control tasks, providing the solver with a better initial guess can expedite the optimization process. This process, known as warm starting, involves initializing the optimization algorithm with a solution that is closer to the optimal solution than a randomly chosen starting point. The intuition behind warm starting is that, at each iteration, the solver refines its solution based on previous iterations. As

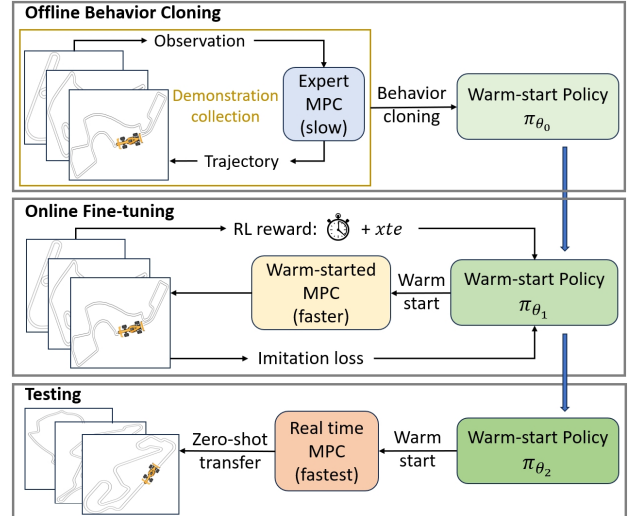


Fig. 1: Overview of our proposed algorithm. The first two blocks denote the two-phase training framework. In the first phase, we collect expert MPC demonstrations and train a warm-start policy using behavior cloning to speed up MPC. In the second phase, we fine-tune this policy within an online training framework to enhance its performance and generalizability. During testing, the proposed framework is evaluated on both training tracks and challenging holdout tracks, as demonstrated in the third block.

shown in Figure 2, a closer initial guess reduces the distance the optimization algorithm needs to traverse to converge to the optimal solution. By starting closer to the optimum, the solver can often avoid lengthy exploration of the solution space, leading to faster convergence and reduced computational effort. In this paper, we choose to test our proposed algorithm to warm start Model Predictive Control (MPC), which optimizes a trajectory over a predefined horizon.

To expedite the optimization process of MPC, various approaches have been adopted. However, they have fallen short on holdout domains, or have limitations in dealing with sudden state changes. Traditionally, one common technique involves utilizing the MPC solution from the previous sampling instance as the initial guess for the current control step [15, 16]. However, this approach falls short when faced with sudden state changes (e.g., the vehicle approaches a sharp turn). Another method involves maintaining a memory buffer to store historical MPC solutions, from which a suitable initial guess can be retrieved for future planning steps [13, 17]. However, this approach may lack zero-shot

*This work was supported by XXXX

1. Georgia Institute of Technology, Atlanta, GA 30332, USA
 2. MIT Lincoln laboratory, Lexington, MA 02421
 3. Ford Motor Company, Dearborn, MI 48120, USA

generalizability. As the system’s state becomes heterogeneous, the size of the memory buffer needs to increase to maintain effectiveness. Moreover, searching for the initial guess within the memory buffer scales at least linearly with its size, potentially causing time-consuming operations. Alternatively, a learning-based methods have been proposed by Klaučo et al. to utilize k-NN classifier to classify the solution space into different active sets from which the solver searches for a solution [18]. However, this method falls short in providing a precise warm-started initial guess and is not capable of dealing with challenging control tasks featuring long planning horizon and heterogeneous observations. Additionally, this approach is limited to solving strictly convex quadratic programs, imposing significant constraints on its applicability and generalizability given that many real-world control problems lack a linear or differentiable objective function and dynamics model. Thus, there is a pressing need for innovative approaches that can effectively address the challenges posed by the inherent complexity and non-linearity of real-world control systems.

In this paper, we propose a two-phase learning framework to learn a warm-start policy that provides a better initial guess for iterative control optimization algorithms (such as MPC) to reduce the optimization time. Our proposed algorithm is depicted in Figure 1, which includes a two-phase training framework and an additional holdout testing phase. An advantage of utilizing a learned policy to initialize the MPC, as opposed to learning a policy for end-to-end control of the system, is that it maintains the integrity of the original problem definition. The learned initial guess solely influences the starting point of the search, without altering the underlying problem setup, while MPC acts as a shield for the learned policy so that the control solution satisfies the constraints of the system, which ensures safer operation of the control system. Moreover, the proposed algorithm enables seamless adaptation to new conditions without the need for extensive retraining. During testing, the warm-start policy is tested on both the training domains and some holdout domains, demonstrating the generalizability of our framework in providing a good initial guess. Our key contributions are:

- 1) Propose a two-phase learning framework featuring offline training and online fine-tuning to learn a warm-start policy that provides the iterative control optimization algorithm with higher-quality initial guesses, aiding the command of a high-speed vehicle on multiple novel, challenging Formula 1 tracks in real-time where traditional warm start methods struggle.
- 2) Empirically evaluate our proposed two-phase learning framework and show the online fine-tuning phase helps the iterative control optimization algorithm achieve a 3.9% higher performance in optimization time and a 3.6% higher performance in tracking accuracy on challenging holdout tracks.

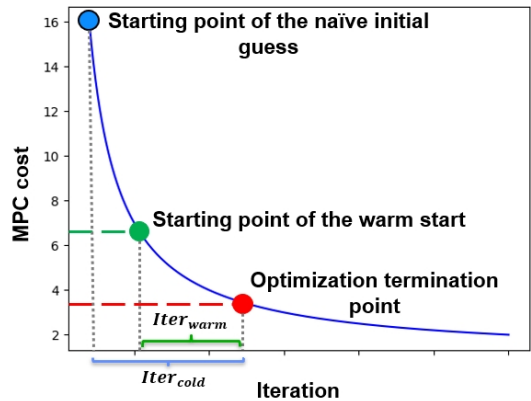


Fig. 2: An illustrative demo showing how a better initial guess improves MPC optimization time.

II. PRELIMINARY

A. Model Predictive Control

Unlike traditional control methods, MPC utilizes a predictive model of the system to anticipate future behavior of the system over a defined planning horizon, H . The control problem is formulated as an optimization task, where the objective is to minimize a cost function while satisfying constraints on the system’s inputs and outputs. This optimization problem is typically solved iteratively at each time step, generating a sequence of control inputs that steer the system towards a desired state while considering future predictions of its behavior. When MPC observes a new state, x_t , at time step, t , it optimizes a sequence of control inputs, U , over the planning horizon by iteratively minimizing a cost function J while respecting system dynamics and constraints. Then, only the first action in the action sequence is applied to the controlled system, which leads the system to the next state. The optimization process is performed again at the next state. The MPC control law is formulated as shown below in Equations (1):

$$J = \underset{U}{\text{minimize}} \sum_{i=0}^{H-1} l(x_{t+i}, u_{t+i}) \quad (1a)$$

$$\text{subject to } x_{t+i+1} = f(x_{t+i}, u_{t+i}) \quad (1b)$$

$$U = [u_t, \dots, u_{t+H-1}] \in \mathcal{U}_j \text{ for all } j = 1, \dots, n_{c_u} \quad (1c)$$

$$X = [x_t, \dots, x_{t+H}] \in \mathcal{X}_j \text{ for all } j = 1, \dots, n_{c_x} \quad (1d)$$

Equation (1a) formulates the objective function of the MPC. H denotes the planning horizon, t is the current step, and, x_{t+i} is the system state at the $t+i$ step. Given the state, x_{t+i} and the control input, u_{t+i} , the system dynamics model predicts the next state, x_{t+i+1} , using the dynamics model (1b). Equation (1c) and Equation (1d) are the constraints for the control inputs and states. n_{c_u} and n_{c_x} are the number of constraints on control inputs and states respectively.

Solvers used to address the above optimization problem can be divided into gradient-based and gradient-free solvers.

Gradient-based solvers leverage the gradient of the cost function with respect to the control inputs to iteratively adjust the control inputs towards the optimal solution [19, 20]. These solvers are effective when the cost function and constraints are smooth and differentiable, while gradient-free solvers do not rely on gradient information for optimization. Instead, gradient-free solvers explore the search space using heuristics, pattern searches, or stochastic techniques to find the optimal solution [19, 20]. To relax the constraints imposed on the problem formulation and demonstrate the generalizability of our framework, we choose to use the gradient-free solver COBYLA [21] in our experiments.

III. METHOD

In this section, we discuss in detail the proposed two-phase training framework. In the first phase, we run the MPC to collect the expert demonstrations, which are represented as state-action pairs. Then, we use behavior cloning to train a warm-start policy to mimic the expert MPC’s solution, as shown in Algorithm 1. The output of warm-start policy is utilized as an initial guess to warm start the MPC and reduce the optimization time. In the second phase, we load the pre-trained trajectory prediction model into an online training framework and fine tune the warm-start policy to address the suboptimality problem caused by behavior cloning and improve the model’s generalizability. The online fine tuning phase is shown in Algorithm 2.

Algorithm 1 Offline Training

- 1: **Input:** expert MPC π^{MPC} with planning horizon H and maximum optimization iteration N_{expert} and all-zero vector $\vec{0}$ as initial guess, environment transition T , number of state-action pairs to collect N
 - 2: Initialize neural network policy $\pi_{\theta}^{\text{warm}}$
 - 3: $t \leftarrow 0, s \leftarrow s_0, \mathcal{D} = \emptyset$
 - 4: **while** $t < N$ **do**
 - 5: $(u_t, u_{t+1}, \dots, u_{t+H-1}) \leftarrow \pi^{\text{MPC}}(s, \vec{0})$
 - 6: $\mathcal{D} \leftarrow \mathcal{D} \cup \{(s, u_t, u_{t+1}, \dots, u_{t+H-1})\}$
 - 7: $s \leftarrow T(s, u_t)$
 - 8: $t \leftarrow t + 1$
 - 9: **end while**
 - 10: Train $\pi_{\theta}^{\text{warm}}$ with Equation (2) and \mathcal{D}
-

A. Offline Training

At this phase, we implement an expert MPC to collect a dataset \mathcal{D} containing N state-action pairs first. The expert MPC, π^{MPC} aims to control the agent to finish the task without relying on a warm-started initial guess for the control action sequence. At each step, π^{MPC} observes a state s and takes an all-zero vector as the initial guess and optimizes that initial guess to output $(u_t, u_{t+1}, \dots, u_{t+H-1})$ (line 5). Then the state-action pair, $(s, u_t, u_{t+1}, \dots, u_{t+H-1})$ is stored in the dataset \mathcal{D} (line 6). The first action in the action sequence is applied to the system, which leads the system to the next state based on the environment transition T (line 7-8). During

Algorithm 2 Online Fine Tuning

- 1: **Input:** fast MPC $\pi_{\text{fast}}^{\text{MPC}}$ with planning horizon H and maximum optimization iteration N_{fast} , environment transition T , pre-trained warm-start policy $\pi_{\theta}^{\text{warm}}$
 - 2: **for** each RL training iteration **do**
 - 3: Perceive an observation s
 - 4: $\hat{U}_t = (\hat{u}_t, \hat{u}_{t+1}, \dots, \hat{u}_{t+H-1}) \leftarrow \pi^{\text{warm}}(s)$
 - 5: $\text{pos}_{i+1}^{\text{car}} = M_{\text{dynamics}}((s_i, \hat{u}_i))|_{i=t}^{H-1}$
 - 6: Compute accumulated xte using Equation (4)
 - 7: $U_t^{\text{MPC}} = (u_t, u_{t+1}, \dots, u_{t+H-1}) \leftarrow \pi_{\text{fast}}^{\text{MPC}}(s, \hat{U}_t)$
 - 8: Calculate reward in RL using Equation (5)
 - 9: $L_{\text{imitation}} = \text{MSE}(U_t^{\text{MPC}}, U_t^{\text{guess}})$
 - 10: Compute training loss L in Equation (3)
 - 11: $s \leftarrow T(s, u_t)$
 - 12: Update $\pi_{\theta}^{\text{warm}}$ with L
 - 13: **end for**
-

the data collection stage, π^{MPC} optimizes the initial guess for enough iterations to make sure it achieves a high control performance by disabling the “early stop” for the expert MPC.

We design our warm-start policy, $\pi_{\theta}^{\text{warm}}$, as a multi-layer perceptron with ReLU activation function [22]. Given the current state of the vehicle, the $\pi_{\theta}^{\text{warm}}$ predicts a sequence of actions which then serves as the initial guess of the MPC to warm start the optimization process. In the offline training phase, we utilize behavior cloning to train $\pi_{\theta}^{\text{warm}}$ (line 10).

Behavior Cloning (BC) is a simple yet effective algorithm to learn from demonstrations. The demonstration is a set of trajectories: $\mathcal{D} = \{\tau_i\}$. BC learns a control policy, π_{θ} , by minimizing the Mean Squared Error (MSE) in the demonstration set, shown in Equation (2). Our algorithm utilizes pre-collected MPC data to perform BC as a warm start for the MPC to improve the MPC’s optimization time.

$$\theta^* = \min_{\theta} \sum_{\tau^i \in \mathcal{D}} \sum_{t=0}^T (\pi_{\theta}^{\text{warm}}(s^i)_t - u_t^i)^2 \quad (2)$$

B. Online Fine Tuning

Our second phase, online fine tuning, further improves the warm-start policy by learning from the data gathered online using the policy trained through behavior cloning. This phase combines the best aspects of Reinforcement Learning and Dataset Aggregation (DAgger) [23] algorithm. Reinforcement Learning (RL) operates under the formalization of Markov Decision Process (MDP), $\mathcal{M} = \langle \mathcal{S}, \mathcal{A}, R, T, \gamma, \rho_0 \rangle$. \mathcal{S} is the state space and \mathcal{A} denotes the action space. R encodes the reward of a given state. T is a deterministic transition function that decides the next state, s' , when applying the action, $a \in \mathcal{A}$, in state, $s \in \mathcal{S}$. $\gamma \in (0, 1)$ is the temporal discount factor. ρ_0 denotes the initial state probability distribution. A policy, $\pi : \mathcal{S} \rightarrow [0, 1]^{|\mathcal{A}|}$, is a mapping from states to actions or to a probability distribution over actions. The objective of RL is to find the

policy that optimizes the expected discounted return, $\pi^* = \mathbb{E}_{\tau \sim \pi} [\sum_{t=0}^{\infty} \gamma^t R(s_t)]$.

Dagger builds upon behavior cloning (BC) by incorporating online interaction with the environment and online querying of the expert. Unlike BC, which trains solely on a fixed dataset of expert demonstrations, DAgger actively collects data from interactions with the environment and solicits expert feedback to augment its training. This online improvement process allows DAgger to learn from a more diverse set of experiences, adapt to new situations, and refine the agent’s policy over time, ultimately leading to improved performance in imitation learning tasks.

In our framework, RL is used to address the sub-optimality and covariance shift problem caused by offline behavior cloning. DAgger, on the one hand, is adopted to regulate the trajectory prediction model during reinforcement learning training, ensuring it does not forget the experience learned from behavior cloning. Further more, DAgger improves the performance of imitation learning by expanding the diversity of the expert MPC’s demonstrations. Given that offline reinforcement learning algorithms require lots of data to effectively cover the entire state space, we choose to fine-tune our pre-trained trajectory prediction model using Proximal Policy Optimization (PPO) [24] as our RL training algorithm. The trajectory prediction model acts as a policy network in the PPO framework. DAgger is integrated as a loss term in the RL training, as shown in Equation (3). L_{RL} is the standard PPO loss which includes three parts: L_{policy} , $L_{entropy}$, and L_{value} . $L_{imitation}$ is the loss signal from DAgger. It represents MSE between the expert MPC’s solution and the warm-started initial guess output from π_{θ}^{warm} . λ is the weight coefficient for the RL loss and imitation loss.

$$\begin{aligned} L &= \lambda \cdot L_{RL} + (1 - \lambda) \cdot L_{imitation} \\ L_{RL} &= \lambda_1 \cdot L_{policy} + \lambda_2 \cdot L_{entropy} + \lambda_3 \cdot L_{value} \end{aligned} \quad (3)$$

$$xte = distance(pos_t^{car}, \mathbf{p}_i(x_i, y_i)^{closest}) \quad (4)$$

In our driving task, the reward at each step of the RL training is shown in Equation (5). The first term is the negative MPC optimization time, and the second term is the negative of the accumulated Cross Track Error (xte) over the planning horizon, H . The xte is defined in Equation (4). At each step, π_{θ}^{warm} will output an action sequence of length H based on the current state vector, s_t . Then, the dynamics model, $M_{dynamics}$, is used to calculate the future positions of the agent. The xte is computed between the reference trajectory and the future positions of the vehicle, pos_i^{car} . The reward obtained at each step directly influences L_{RL} by contributing to the calculation of the advantage estimate, which measures the discrepancy between the observed reward and the expected value of the state-action pair. This estimate affects both L_{policy} , which encourages actions leading to higher rewards, and L_{value} , which trains the value function to better estimate cumulative rewards.

$$r_t = -time_{MPC} - \sum_{i=t+1}^{t+H} xte(pos_i^{car}, Traj^{ref}) \quad (5)$$

This reward design helps to optimize the π_{θ}^{warm} by minimizing the MPC running time and by minimizing the difference between the planned trajectory and the reference trajectory, thereby reducing MPC optimization time. This helps to address the sub-optimality problem caused by behavior cloning.

IV. EXPERIMENTS

In this section, we will discuss in detail the setup of the Formula 1 tracks domains, followed by the MPC design in this testing domain. Additionally, we will present experimental results from both training and holdout tracks, demonstrating how our algorithm enhances MPC’s performance in terms of both optimization time and tracking accuracy.

A. Experiment Setup

The experiments are done in high-speed Formula 1 tracks [25] which are divided into three training tracks and seven zero-shot testing tracks, as shown in Figure 3a, Figure 3b, and Figure 3c, respectively. The reference trajectory is represented as a set of waypoints in the center of the track. The track size is downscaled to a 10:1 ratio to make each lap a reasonable length. The reference speed for the vehicle in the expert MPC is $10m/s$. Given the downscaled size of the track data, the vehicle could actually speed up to $100m/s$ in the 1:1 scale track. The friction between the tire and the road is not considered in our dynamics model, as it depends on multiple factors such as tire pressure, temperature, humidity, and road conditions. The path tracking is challenging for traditional gradient-free MPC because the vehicle is running at a high speed and the tracks have multiple sharp turns. In this scenario, traditional gradient-free MPC solvers could not optimize the control solution in real time, which makes it unreasonable for real-world application.

The three tracks used for demonstration collection and training are shown in Figure 3a. The six zero-shot tracks are not presented to the vehicle before testing to demonstrate our algorithm’s zero-shot generalizability. During training, the expert MPC is first rolled out on training tracks to collect demonstrations for offline training introduced in Section III-A. Then, the warm-start policy is fine-tuned on the same three tracks using the algorithm introduced in Section III-B.

As shown in Figure 2, without a specified threshold, optimization continues until reaching the maximum iteration limit. In our experiments, we found that the MPC cost reduces subtly during the later optimization iterations. As such, it is important to provide the solver with an early-stop criterion. We implement the early-stop condition based on a planned trajectory’s accumulated cross-track error (xte) being $< 0.1m$. Additionally, to ensure real-time planning during testing, we cap the maximum optimization iterations at 50, which guarantees that the optimization time is less than 0.08 seconds in worst-case scenarios. Details of the

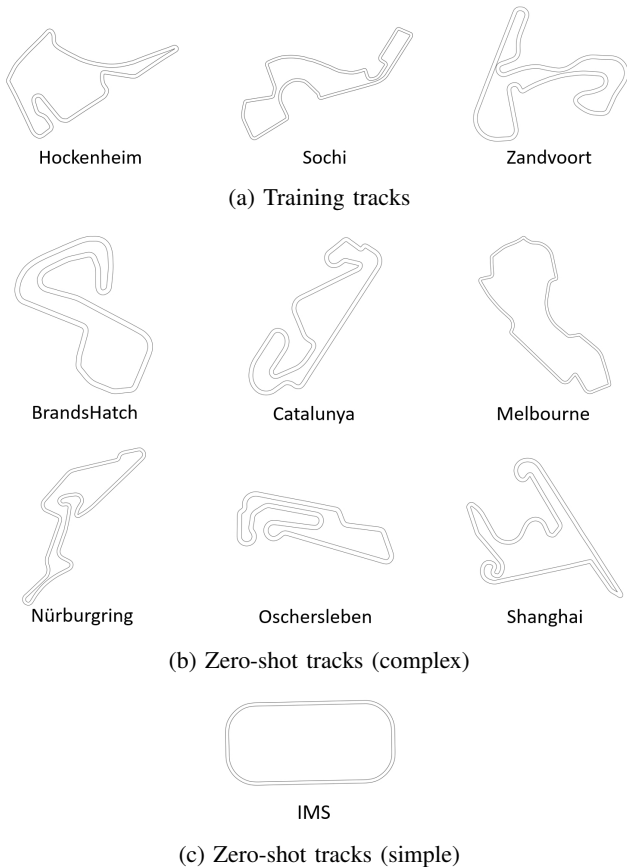


Fig. 3: Tracks tested during training and testing.

MPC design and hyper parameters in MPC and training are presented in Appendix VI-A and VI-B

B. Experiment Results

During testing, we evaluate on two metrics: the average MPC optimization time (seconds) per step and the average xte (m) per step. We benchmark our algorithm’s performance against MPC using all-zero initial guesses and initial guesses derived from the MPC’s solution at the previous step. We perform testing on both the training tracks (Figure 3a) and the challenging zero-shot tracks (Figure 3b). The results are shown in Figure 4 and Figure 5, respectively.

1) *Optimization Time*: On both the training and zero-shot tracks, employing a warm-start policy trained through either offline learning or a combination of offline and online fine-tuning significantly reduces MPC optimization time, falling well within the upper bound of $0.08s$. Additionally, the warm-start policy trained with both offline and online fine-tuning achieves better MPC optimization time compared to the policy trained solely through offline behavior cloning, demonstrating the capability of our online fine-tuning algorithm in addressing the suboptimality problem caused by behavior cloning (BC). Furthermore, our two-phase training framework achieves more significant improvement in the zero-shot domains, indicating that the online fine-tuning phase alleviates the covariance shift problem caused by BC

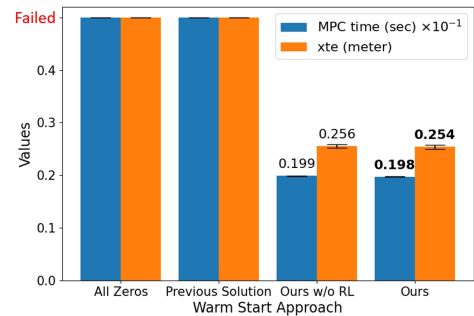


Fig. 4: Experiment results on training tracks.

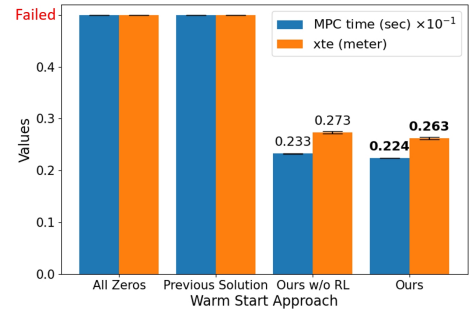


Fig. 5: Experiment results on the six zero-shot testing tracks.

and enhances the model’s generalizability.

2) *Control Performance (xte)*: In the context of the training tracks, the warm-start policy trained through offline and online fine-tuning outperforms the policy trained solely through offline behavior cloning in terms of tracking accuracy, further illustrating the effectiveness of our online fine-tuning algorithm in addressing the suboptimality problem caused by BC. Given that the width of the downscaled track is $2.2m$, achieving an xte of less than $0.3m$ demonstrates precise tracking of the reference path. Additionally, our two-phase training framework exhibits more significant improvement in the zero-shot domains, reinforcing the efficacy of the online fine-tuning phase in mitigating the covariance shift problem caused by BC and improving the model’s generalizability.

The results also reveal that employing an MPC with either an all-zero initial guess or an initial guess derived from the MPC’s previous solution fails to complete laps on both the training and zero-shot tracks. The vehicle consistently deviates from the lane and struggles to navigate sharp turns. This limitation arises because the MPC often requires more iterations to optimize the control solution as the vehicle approaches the curves of the track. Since the real-time MPC only optimizes the solution for a maximum of 50 iterations at each step, the returned solution lacks the optimization necessary to guide the vehicle through sharp turns effectively. This underscores the necessity of a well-informed initial guess to minimize the number of optimization iterations required.

As the real-time MPC with either an all-zero initial guess or an initial guess derived from the MPC’s previous solution

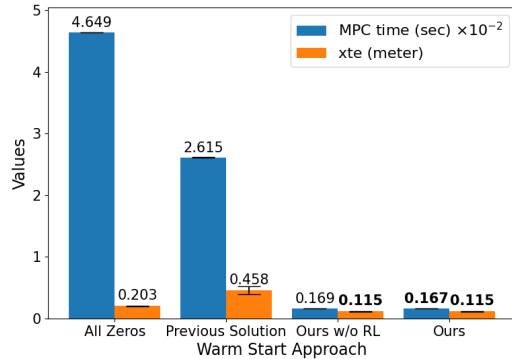


Fig. 6: Experiment results on the simple IMS track.

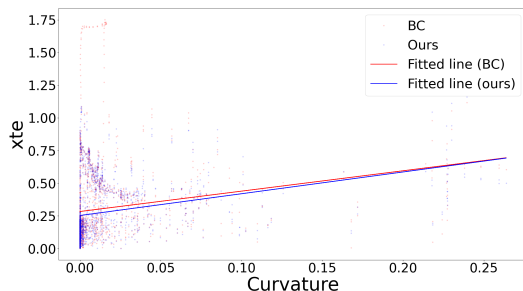


Fig. 7: We run the MPC with two types of warm-start policy (BC and ours) on the "Catalunya" track, where we gather data on the xte and track curvature surrounding the vehicle. Subsequently, we depict these data points in the figure above.

fails to complete laps on both the training and challenging zero-shot tracks, we conducted further testing on four warm start policies on a simple zero-shot track, IMS, as depicted in Figure 3c. The results are summarized in Figure 6. Our method demonstrates a significant reduction in MPC optimization time while maintaining high tracking accuracy, showcasing its effectiveness in enhancing MPC performance.

As the vehicle route on the track, we further compute the curvature of the track surrounding the vehicle. This analysis allows us to illustrate the correlation between the curvature and lateral error (xte), depicted in Figure 7. It shows that our second phase fine tuning has an advantage on average xte and this advantage has a modest increase when the track is less curvy. This outcome underscores the efficacy of our proposed algorithm in enhancing the precision of the planned trajectory. Details regarding the method employed to compute the curvature of the track around the vehicle are provided in the Appendix VI-C

In summary, our empirical results support that:

- MPC with initial guesses trained by data-driven methods significantly outperforms those with all-zero or previous solution-derived guesses, crucial for navigating sharp turns.
- The warm-start policy trained with our two-phase learning framework reduces MPC optimization time and

xte on both training and zero-shot tracks, showing the capability of our online fine-tuning algorithm in addressing the suboptimality problem.

- The two-phase training shows superior performance in zero-shot scenarios, indicating better generalizability.

V. LIMITATIONS AND FUTURE WORKS

While our proposed two-phase learning framework shows promising results in expediting optimization processes and enhancing control performance for robot control tasks, there are several limitations and avenues for future research that merit consideration. One limitation of our current experiments is that we have only focused on autonomous driving where the action space is limited to two dimensions (i.e., steering and acceleration). Future work could expand into more complex domains, such as robot arm manipulation or quadcopter control, to explore the algorithm's efficacy in higher-dimensional spaces. Additionally, future research could also involve utilizing our proposed algorithm to expedite other iterative control optimization techniques like MPPI. Although our algorithm primarily interfaces with MPC, it is versatile enough to serve as a warm start for other iterative control optimization methods like Model Predictive Path Integral (MPPI) control [26]. MPPI typically employs stochastic optimization, initializing with a guess of the control sequence distribution, sampling sequences, and iteratively refining the distribution to minimize control cost. Our framework can be trained to predict the trajectory Gaussian distribution mean, enhancing MPPI's performance by offering a superior initial distribution. This reduces the iteration count needed for optimization, aligning with early stopping criteria. While MPC suits systems with complex dynamics and constraints, we choose it as our focus due to its representativeness in trajectory optimization methods.

VI. CONCLUSIONS

In this paper, we introduce a novel approach to accelerate MPC optimization by learning a warm-start policy. Our two-phase learning framework combines offline behavior cloning and online fine-tuning to provide improved initial guesses for the MPC solver. Experimental results on both training and zero-shot tracks demonstrate the effectiveness of our approach in reducing optimization time and enhancing path tracking accuracy. Our learning framework integrated with MPC opens up new avenues for improving the efficiency and applicability of trajectory optimization in various dynamic systems.

APPENDIX

A. MPC Design Details

MPC is designed to control the acceleration and the steering of the vehicle to track the reference trajectory. The dynamics model of the vehicle, $M_{dynamics}$, is shown in Equation (6). (x_t^{car}, y_t^{car}) is the global position of the vehicle at time step t . v_t and yaw_t are the speed (m/s) and yaw angle (rad) of the vehicle at time step t . a_t and $\theta_t^{steering}$ are acceleration (m/s^2) and steering angle (rad) inputs to the

vehicle at time step t . L is the wheelbase of the vehicle. Here we use Ford Mustang’s dimensions, $L = 2.89m$. And $dt = 0.02$ is the length of each time step which represents the duration between successive updates of control inputs and system states.

$$x_{t+1}^{car} = x_t^{car} + v_t \cdot \cos(yaw_t) \cdot dt \quad (6a)$$

$$y_{t+1}^{car} = y_t^{car} + v_t \cdot \sin(yaw_t) \cdot dt \quad (6b)$$

$$yaw_{t+1} = yaw_t + \frac{v_t}{L} \cdot \tan(\theta_t^{\text{steering}}) \cdot dt \quad (6c)$$

$$v_{t+1} = v_t + a_t \cdot dt \quad (6d)$$

The MPC objective function is composed of five parts as shown in Equation (7). The first two terms are *xte* and Error in Heading (*eth*). *xte* is computed using Equation 4. *eth* denotes the angular disparity between the intended path direction and the current heading of a vehicle in path tracking systems. And *eth* is computed using Equation (8). v_t^{ref} is the desired speed of the vehicle. The last two terms in Equation (7) regulate the rate of change of the steering angle and acceleration to make planned trajectory smoother. w_0, w_1, w_2, w_3, w_4 are the coefficients balancing the importance of each term. The planning horizon of the MPC is 25 steps and the planning step dt is 0.02 seconds, which means that the MPC looks 0.5 seconds ahead.

$$J_t = \sum_{i=t}^{t+H-1} (w_0 \cdot xte_i^2 + w_1 \cdot eth_i^2 + w_2 \cdot (v_i - v_t^{\text{ref}})^2 + w_3 \cdot (steer_i - steer_{i-1})^2 + w_4 \cdot (throttle_i - throttle_{i-1})^2) \quad (7)$$

$$eth = abs \left(yaw_t^{car} - \arctan \left(\frac{y_{i+1} - y_i}{x_{i+1} - x_i} \right) \right) \quad (8)$$

B. Hyper Parameters in MPC and Training

Hyperparameters	Values
Weight in MPC cost function w_0	2000
Weight in MPC cost function w_1	100
Weight in MPC cost function w_2	60
Weight in MPC cost function w_3	2
Weight in MPC cost function w_4	20
Weight in MPC cost function w_5	300
Loss weight coefficient λ	0.9
Loss weight coefficient λ_1	0.5
Loss weight coefficient λ_2	0
Loss weight coefficient λ_3	0.5
MPC planning horizon	25
Length of each time step	0.02 second
Reference speed	10m/s
Wheelbase	2.89 m
Expert MPC maximum optimization iteration	300
Real-time MPC maximum optimization iteration	300
Real time MPC early stop criteria	$xte < 0.1$

C. Curvature Computation

Algorithm 3 Curvature Computation

- 1: Extract 10 consecutive nearest waypoints ahead of the vehicle, $\mathbf{P} = \{\mathbf{p}_1, \mathbf{p}_2, \dots, \mathbf{p}_{10}\}$. $\mathbf{p}_i = (x_i, y_i)$ represent the i -th waypoint
- 2: **for** \mathbf{p}_{i-1} , \mathbf{p}_i , and \mathbf{p}_{i+1} in \mathbf{P} **do**
- 3: Compute the vector $\mathbf{v}_1 = \mathbf{p}_i - \mathbf{p}_{i-1}$
- 4: Compute the vector $\mathbf{v}_2 = \mathbf{p}_{i+1} - \mathbf{p}_i$
- 5: Calculate the dot product $\mathbf{v}_1 \cdot \mathbf{v}_2$
- 6: Calculate the magnitudes $\|\mathbf{v}_1\|$ and $\|\mathbf{v}_2\|$
- 7: Compute the cos of the angle between the vectors:

$$\cos(\theta_i) = \left(\frac{\mathbf{v}_1 \cdot \mathbf{v}_2}{\|\mathbf{v}_1\| \|\mathbf{v}_2\|} \right)$$

8: **end for**

9: *Curvature* = $\sum_{i=2}^9 (1 - \cos(\theta_i))$

REFERENCES

- [1] Francesco Borrelli et al. “MPC-based approach to active steering for autonomous vehicle systems”. In: *International journal of vehicle autonomous systems* 3.2-4 (2005), pp. 265–291.
- [2] Napat Karnchanachari et al. “Practical Reinforcement Learning For MPC: Learning from sparse objectives in under an hour on a real robot”. In: *Learning for Dynamics and Control*. PMLR. 2020, pp. 211–224.
- [3] Jason Kong et al. “Kinematic and dynamic vehicle models for autonomous driving control design”. In: *2015 IEEE intelligent vehicles symposium (IV)*. IEEE. 2015, pp. 1094–1099.
- [4] Taekyung Kim et al. “Smooth model predictive path integral control without smoothing”. In: *IEEE Robotics and Automation Letters* 7.4 (2022), pp. 10406–10413.
- [5] Leonard Bauersfeld et al. “MPC flight control for a tilt-rotor VTOL aircraft”. In: *IEEE Transactions on Aerospace and Electronic Systems* 57.4 (2021), pp. 2395–2409.
- [6] Ali Jadbabaie and John Hauser. “Control of a thrust-actuated flying wing: a receding horizon—LPV approach”. In: *International Journal of Robust and Non-linear Control: IFAC-Affiliated Journal* 12.9 (2002), pp. 869–896.
- [7] Scott Kuindersma et al. “Optimization-based locomotion planning, estimation, and control design for the atlas humanoid robot”. In: *Autonomous robots* 40 (2016), pp. 429–455.
- [8] Jacob Sacks and Byron Boots. “Learning sampling distributions for model predictive control”. In: *Conference on Robot Learning*. PMLR. 2023, pp. 1733–1742.
- [9] James B Rawlings, Edward S Meadows, and Kenneth R Muske. “Nonlinear model predictive control: A tutorial and survey”. In: *IFAC Proceedings Volumes* 27.2 (1994), pp. 185–197.

- [10] Utku Eren et al. “Model predictive control in aerospace systems: Current state and opportunities”. In: *Journal of Guidance, Control, and Dynamics* 40.7 (2017), pp. 1541–1566.
- [11] Mohamed-Khalil Bouzidi et al. “Learning-Aided Warmstart of Model Predictive Control in Uncertain Fast-Changing Traffic”. In: *arXiv preprint arXiv:2310.02918* (2023).
- [12] Teguh Santoso Lembono et al. “Learning how to walk: Warm-starting optimal control solver with memory of motion”. In: *2020 IEEE International Conference on Robotics and Automation (ICRA)*. IEEE, 2020, pp. 1357–1363.
- [13] Nicolas Mansard et al. “Using a memory of motion to efficiently warm-start a nonlinear predictive controller”. In: *2018 IEEE International Conference on Robotics and Automation (ICRA)*. IEEE, 2018, pp. 2986–2993.
- [14] Stefan Richter, Colin N Jones, and Manfred Morari. “Real-time input-constrained MPC using fast gradient methods”. In: *Proceedings of the 48th IEEE Conference on Decision and Control (CDC) held jointly with 2009 28th Chinese Control Conference*. IEEE, 2009, pp. 7387–7393.
- [15] Melanie Nicole Zeilinger, Colin Neil Jones, and Manfred Morari. “Real-time suboptimal model predictive control using a combination of explicit MPC and online optimization”. In: *IEEE Transactions on Automatic Control* 56.7 (2011), pp. 1524–1534.
- [16] Yunpeng Pan et al. “Imitation learning for agile autonomous driving”. In: *The International Journal of Robotics Research* 39.2-3 (2020), pp. 286–302.
- [17] Tobia Marcucci and Russ Tedrake. “Warm start of mixed-integer programs for model predictive control of hybrid systems”. In: *IEEE Transactions on Automatic Control* 66.6 (2020), pp. 2433–2448.
- [18] Martin Klaučo, Martin Kalúz, and Michal Kvasnica. “Machine learning-based warm starting of active set methods in embedded model predictive control”. In: *Engineering Applications of Artificial Intelligence* 77 (2019), pp. 1–8.
- [19] Jay H Lee. “Model predictive control: Review of the three decades of development”. In: *International Journal of Control, Automation and Systems* 9 (2011), pp. 415–424.
- [20] Max Schwenzer et al. “Review on model predictive control: An engineering perspective”. In: *The International Journal of Advanced Manufacturing Technology* 117.5 (2021), pp. 1327–1349.
- [21] Michael JD Powell. *A direct search optimization method that models the objective and constraint functions by linear interpolation*. Springer, 1994.
- [22] Xavier Glorot and Yoshua Bengio. “Understanding the difficulty of training deep feedforward neural networks”. In: *Proceedings of the thirteenth international conference on artificial intelligence and statistics*. JMLR Workshop and Conference Proceedings, 2010, pp. 249–256.
- [23] Stéphane Ross, Geoffrey Gordon, and Drew Bagnell. “A reduction of imitation learning and structured prediction to no-regret online learning”. In: *Proceedings of the fourteenth international conference on artificial intelligence and statistics*. JMLR Workshop and Conference Proceedings, 2011, pp. 627–635.
- [24] John Schulman et al. “Proximal policy optimization algorithms”. In: *arXiv preprint arXiv:1707.06347* (2017).
- [25] *fltenth-racetracks*. https://github.com/fltenth/fltenth_racetracks.
- [26] Grady Williams, Andrew Aldrich, and Evangelos Theodorou. “Model predictive path integral control using covariance variable importance sampling”. In: *arXiv preprint arXiv:1509.01149* (2015).